Original Research Paper

Open Access

The Use of Cobalt-Doped Tin(IV) Oxide as a Catalyst for the Photodegradation of Methyl Orange

Anti Kolonial Prodjosantoso† and Cahyorini Kusumawardani
Department of Chemistry, Yogyakarta State University, Yogyakarta, 55281, Indonesia
†Corresponding author: Anti Kolonial Prodjosantoso

ABSTRACT

Textile industries are always deal with water pollution caused by pigments, one of which is organic compounds. Efforts have been made to treat the polluted water, however the methods still need to be improved. Cobalt-doped tin(IV) oxide ($Sn_{1-x}Co_xO_2$, x = 0, 0.0025 and 0.005) prepared by a solid state reaction of SnO_2 powder and cobalt nitrate salt has been introduced to catalysis of methyl orange photodegradation. The catalysts have band gap energy (E_g) varied between 1.813 and 3.944 eV, and indicates good responses in both visible and ultraviolet lights, having high potent as photocatalysts on methyl orange degradation. The test indicates the applicability of Langmuir adsorption isotherm for the systems.

INTRODUCTION

The biggest problem with textile industries, for example, is dyes (Carmen & Daniel 2012). The dyes may poison water organisms, and block sunlight to penetrate water, disturbing the process of photosynthesis. The textile dyes are hardly decomposed causing disruption of water ecosystems for a long period of time (Ito et al. 2016).

The polluted water recovery process is very complicated, high cost and time consuming. The problem is more complex if the dyes settled in the water are toxic, carcinogenic, and mutagenic (Alves de Lima et al. 2007, Jäger et al. 2006). Many dyes are azo compounds which are nondegradable, and endanger living organisms (Cisneros et al. 2002, Ozdemir et al. 2013, Ribeiro & Umbuzeiro 2014). One of the azo dyes used in colouring textile is methyl orange (MO) which is a cationic heterocyclic aromatic compound (Li et al. 2013).

Dye removal from water includes conventional methods such as adsorption using activated carbon or zeolites, and modern methods, such as biodegradation, ozonization, chlorination, ionizing radiation and plasma technology. The conventional methods are less applicable and ineffective to use, while modern methods are usually expensive (Ozdemir et al. 2013, Robinson et al. 2002, Samad et al. 2016, Vidal et al. 2016).

Photodegradation, the environmental friendly and low cost method, may be applied to decompose the dyestuff wastes. Photodegradation may be facilitated by using photocatalysts. Photocatalysis combines photochemical processes and catalysis. This process includes chemical transformation process using photons as energy sources and catalysts accelerating the rate of transformation. The process is based on the dual capability of a semiconductor material (such as TiO_2, ZnO, Fe_2O_3, CdS, ZnS) to absorb photons and simultaneously transform the material interface (Banerjee et al. 2014, Ohtani 2011). The use of this photocatalyst has the advantage of being able to totally mineralize the organic pollutants including textile waste (azo compounds), the operational cost is inexpensive with a relatively fast, non-toxic and long-term use, and environmental friendly and reusable (Ohtani 2010). Photocatalyst that is widely used is TiO_2 due to its high activity and band gap energy of 3.2 eV. The use of SnO_2 instead of TiO_2 is of interest (Zheng et al. 2016). The tin oxide photocatalyst having band gap energy of 3.6 eV is enhanced by cobalt oxide so that the catalysts may also work well under visible light (Barakat et al. 2008, Patil 1996, Prodjosantoso et al. 2017a). This stable catalyst may be prepared using arrange of methods, but the high temperature reaction is the simplest and cheapest method (De Almeida et al. 2014).

We are reporting the use of $Sn_{1-x}Co_xO_2$ (x = 0, 0.0025 and 0.005) to catalyse the degradation of methyl orange (MO) solution under UV and visible light radiations.

MATERIALS AND METHODS

Materials: SnO_2 (Merck), $Co(NO_3).6H_2O$ (Merck), and MO

(Sigma-Aldrich) were used as received without any further purification.

Methods: A total of 1.5071 grams of SnO_2 was thoroughly mixed with 0.00728 gram (2.5 x 10^{-5} mol) $Co(NO_3)_2.6H_2O$, and followed by calcination at 900°C for 4 hours. The work was repeated using 0.01455 g (5 x 10^{-5} mol) $Co(NO_3)_2.6H_2O$. The resulting catalysts were then characterized using UV-Vis Spectroscopy (UV-2450PC Pharmaspec Spectrophotometer) method.

The adsorption behaviour of $Sn_{1-x}Co_xO_2$ (x = 0, 0.0025 and 0.005) was determined as follows: a set of adsorption test was performed in the dark, in which 10 mL of MO solutions with different initial concentrations were added with 0.1 g of $Sn_{1-x}Co_xO_2$ (x = 0, 0.0025 and 0.005) powders, and shaken for 24 hours. The MO concentration in the suspensions before and after the adsorption were analysed to determine the amount of MO adsorbed by the catalyst.

The photocatalytic activity of $Sn_{1-x}Co_xO_2$ (x = 0, 0.0025 and 0.005) was determined by measuring the undecomposed MO after being exposed under visible or UV-light. The initial concentration of MO was 1×10^{-5} M. The undecomposed MO at given time intervals was measured using a spectrometry at the absorbance of 462 nm.

RESULTS AND DISCUSSION

UV-Vis spectroscopy method was used to determine the band gap energy of the material, and the absorbances. Prior to the measurements, the $Sn_{1-x}Co_xO_2$ (x = 0, 0.0025 and 0.005) was dissolved in a mixture of triton-x and acetylacetonate to form a paste, which was then layered on the preparatory glass. Furthermore, the glass was dried in a furnace at a temperature of 450°C for 2 hours to evaporate the solvent.

In this study, measurements were carried out at wavelengths of 200-800 nm. Each sample has absorbed energy at certain wavelength(s) (Table 1).

Table 1: Absorbances of $Sn_{1-x}Co_xO_2$.

$Sn_{1-x}Co_xO_2$, x =	λ (nm)	
	Visible	UV
0	-	317
0.0025	405	275 and 315
0.005	395	295

Table 2: The band gap energy of $Sn_{1-x}Co_xO_2$.

$Sn_{1-x}Co_xO_2$, x =	Band Gap Energy (eV)		
	E_g1	E_g2	E_g3
0	3.944	-	-
0.0025	3.819	2.588	1.829
0.005	3.931	2.236	1.813

The Kubelka-Munk equation was used to calculate the band gap energy (E_g) of catalysts (Yang & Kruse 2004). Table 2 lists the band gap energies of $Sn_{1-x}Co_xO_2$ (x = 0, 0.0025 and 0.005). The cobalt, which is doped onto SnO_2, decreases the band gap energy of SnO_2 (3.944 eV) (Prodjosantoso et al. 2017b, Reimann & Steube 1998, Viter et al. 2014). In general, the more cobalt additions provide the lower band gap energy of $Sn_{1-x}Co_xO_2$ (x = 0, 0.0025 and 0.005).

The $Sn_{1-x}Co_xO_2$ (x = 0, 0.0025 and 0.005) photocatalyst adsorption test was performed in the dark environment. Prior to adsorption, the measurement of MO absorbance at a wavelength of 462 nm was performed, to obtain a MO standard curve. The adsorption process used 0.05 grams of catalyst of $Sn_{1-x}Co_xO_2$ (x = 0, 0.0025 and 0.005), and the concentrations of MO were 2, 4, 6, 8 and 10 ($\times10^{-6}$ mol/L). The adsorption of MO by the catalyst was carried out for 24 hours in a closed shaker to obtain a state of equilibrium. Furthermore, the mixture of the degraded solution was centrifuged at a rate of 1500 rpm for 10 minutes to separate the liquid phase from the precipitate. The filtrate was analysed at wavelength of 462 nm to determine the concentration of MO.

The calculation of catalyst adsorption capacity was performed using Langmuir and Freundlich equations (LeVan & Vermeulen 1981). The Langmuir isotherm pattern was determined by correlating the MO concentration adsorbed on every 1 gram of catalyst (c/m) with MO concentration after 24 h (c). The calculation of the adsorption capacity value (b) on the Langmuir isotherm was undertaken using the equation as follows:

$$\frac{c}{m} = \frac{c}{b} + \frac{1}{K_L b} \qquad ...(1)$$

Freundlich isotherm pattern is determined by plotting the log value of the amount of MO adsorbed on every 1 gram of catalyst (log x/m) with the log of MO concentration after 24 hours (log c). The calculation of the adsorption capacity (k) of the Freundlich isotherm was undertaken using equation as follows:

$$\log \frac{x}{m} = \log k + \frac{1}{n} \log c \qquad ...(2)$$

The equations of Langmuir and Freundlich isotherms are presented in Table 3.

The R^2 values of the Langmuir adsorption isotherm pattern are higher than that of the Freundlich. Thus, we can conclude that adsorption on MO degradation by $Sn_{1-x}Co_xO_2$ catalysts follows Langmuir isotherm pattern. This pattern assumes the monolayer formation of adsorbate on the homogenous adsorbent surface. There is no interaction

Table 3: Equations of Langmuir and Freundlich isotherm patterns of $Sn_{1-x}Co_xO_2$.

$Sn_{1-x}Co_xO_2$; x =	Langmuir	Freundlich
0	$y = 0.77253x - 1.29567$ $R^2 = 0.98349$	$y = -0.90112x - 12.05405$ $R^2 = 0.93153$
0.0025	$y = 0.60214x - 1.25004$ $R^2 = 0.96149$	$y = -1.01961x - 12.62908$ $R^2 = 0.81312$
0.005	$y = 0.33124x - 0.55717$ $R^2 = 0.98578$	$y = -2.34525x - 20.64722$ $R^2 = 0.85533$

among the adsorbed molecules, i.e. MO.

The adsorption capacity can be calculated using Langmuir isotherm equation, that is the 1/slope of the line equation. The adsorption capacities of the sample is presented in Table 4. The SnO_2 indicates the lowest adsorption capacity. This is due to SnO_2- supported cobalt oxide having a larger surface and a greater ability to adsorb MO than pure SnO_2.

The photodegradation was performed using 0.05 gram $Sn_{1-x}Co_xO_2$ for every 10 mL of 15.63 ppm MO solution. The mixtures were placed in a shaker covered by a closed box equipped with Evaco 20 Watt fluorescent light. Measurements were undertaken at variations of time i.e., 4, 8.12, 16, 20 and 30 minutes. The absorbances were measured at a wavelength of 462 nm. The absorbances were then referred into the standard MO curve equation to obtain the MO concentration (Fig. 1).

Fig. 1. shows that the concentration of MO decreases with increasing exposed time to UV light. This proves that MO degradation is effectively performed by using $Sn_{1-x}Co_xO_2$ catalysts, under UV light. Fig. 1 also indicates that the SnO_2 catalysed more effectively in degrading the MO compared to $Sn_{1-x}Co_xO_2$ with x = 0.0025 and 0.005, which is similar to results performed by cobalt(II) oxide supported onto tin(IV) oxide catalysts (Cerri et al. 2005).

Fig. 1., however, also shows that the little MO increase after photodegradation for 80 and 120 minutes. It might be a photolysis product appearing which absorbs at the wavelength where the MO concentration is measured, or it might be a simple error in the measurement. In principle, it also might be the consequence of the liberation of adsorbed MO due to co-adsorption of decomposition products, but the increase in the concentration is well enough.

Photodegradation of MO under visible light was undertaken using the same procedure for MO photodegradation under UV light, but the light source used was Philips ML 100W/220-230E27. The absorbances observed were then referred into the standard MO curve equation to obtain the MO concentration (Fig. 2).

Fig. 2 indicates that the concentration of MO solution is inversely proportional to the exposure time of visible light. The catalysts show a good performance under visible light. The performance of $Sn_{1-x}Co_xO_2$ with x = 0.005 in degrading MO is better compared to the SnO_2 and $Sn_{1-x}Co_xO_2$ with x = 0.0025 catalysts.

The reaction order was determined to study the reaction rate kinetics of the MO photodegradation. The largest value of R^2 was used to determine the order of reactions. The zero-order reaction was determined by integrating the equation of the reaction rate, as follows:

$$C_t = -kt + C_0 \qquad ...(3)$$

Where, C_t is the concentration of MO at time t, k is the rate constant, t is time and C_0 is the initial concentration of MO. By plotting C_t vs. t, we obtain the equation of the line for the zero-order reaction, and the R^2 value can be determined.

The first-order reaction was determined by integrating the rate of reaction to obtain the equation of the reaction, as follows:

$$\ln(C_t/C_o) = -kt \qquad ...(4)$$

$$\ln C_t = -kt + \ln C_0 \qquad ...(5)$$

By plotting $\ln C_t$ vs. t, we obtain the equation of the line for the first-order reaction, and the R^2 value can be determined.

The second-order reaction was determined by integrating the rate of reaction to obtain the equation of the reaction, as follows:

$$\frac{1}{C_t} = kt + \frac{1}{C_0} \qquad ...(6)$$

By plotting $1/C_t$ vs. t, we obtain the equation of the line for the second-order reaction.

By comparing the values of R^2 of the three reaction orders (Table 5), the rate of MO photodegradation reaction using catalysts $Sn_{1-x}Co_xO_2$ under UV light and visible light is

Table 4: Adsorption Capacity of $Sn_{1-x}Co_xO_2$.

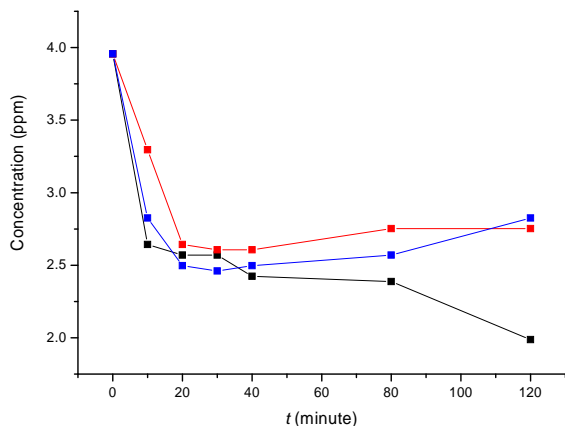| $Sn_{1-x}Co_xO_2$, x=	Adsorption Capacity (mole/gram)
0	1.29444811
0.0025	1.660743349
0.005	3.018959063

Fig. 1: Photoactivity of $Sn_{1-x}Co_xO_2$ with x = 0 (black), 0.0025 (red) and 0.005 (blue) on MO photodegradation under UV light.
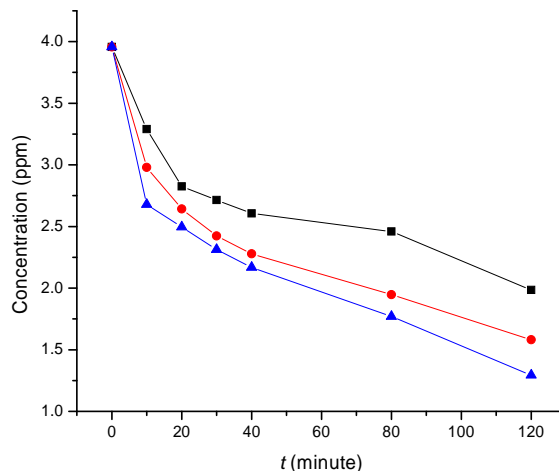

Fig. 2: Photoactivity of $Sn_{1-x}Co_xO_2$ with x = 0 (black), 0.0025 (red) and 0.005 (blue) on MO photodegradation under visible light.

determined. As the second-order kinetics curve has the highest R^2 value than that of zero and first-order, so the order of the reaction is confirmed to be second-order reaction.

The decrease of the concentration of MO in the degradation process using $Sn_{1-x}Co_xO_2$, under UV light and visible light can be seen in Fig. 3.

In the MO degradation experiment using UV irradiation, SnO_2 catalysis is more effective than other catalysts. But, the $Sn_{1-x}Co_xO_2$ performs conversely, and the $Sn_{1-x}Co_xO_2$ with x = 0.005 indicates the most effective catalysis compared to the rest of catalysts. This is because the undoped SnO_2 has a band gap energy working only on UV light, while $Sn_{1-x}Co_xO_2$ works on both UV and visible light.

The photocatalytic reaction takes place in a heterogeneous system and the reaction rate is affected by the adsorbance of the reactants on the surface of the catalyst. Reaction rate can be formulated as follows:

$$r = -\frac{dC}{dt} = \frac{k_{obs}.K.C}{1 + K.C} \qquad ...(7)$$

The reaction rate equation can be simplified into second-order kinetics as follows:

$$\frac{1}{c} = -k_{obs}t + \frac{1}{C_0} \qquad ...(8)$$

Where, k_{obs} is the total reaction rate constant (min^{-1}), K is the adsorption constant of the reactant and C is the concentration of the reactant at any time. Kinetic constant k_{obs} is the rate constant of the reaction, which does not take into account the role of adsorption, so that when the adsorption process becomes the part affecting the photodegradation reaction, it is necessary to determine the actual reaction rate constant (k) that has corrected the k_{obs} with the adsorption constant (K), where $k_{obs} = kKL$.

Kinetics parameter k_{obs} was determined by plotting $1/C_t$ vs t followed by the calculation based on the second-order reaction. The reaction rate constant (k) is determined based on the k_{obs}, and the results can be seen in Table 6.

Table 6 shows that for the $Sn_{1-x}Co_xO_2$ with x = 0 catalyst the magnitude of the reaction rates of MO photodegradation

Table 5: Kinetical data of MO photodegradation reaction order.

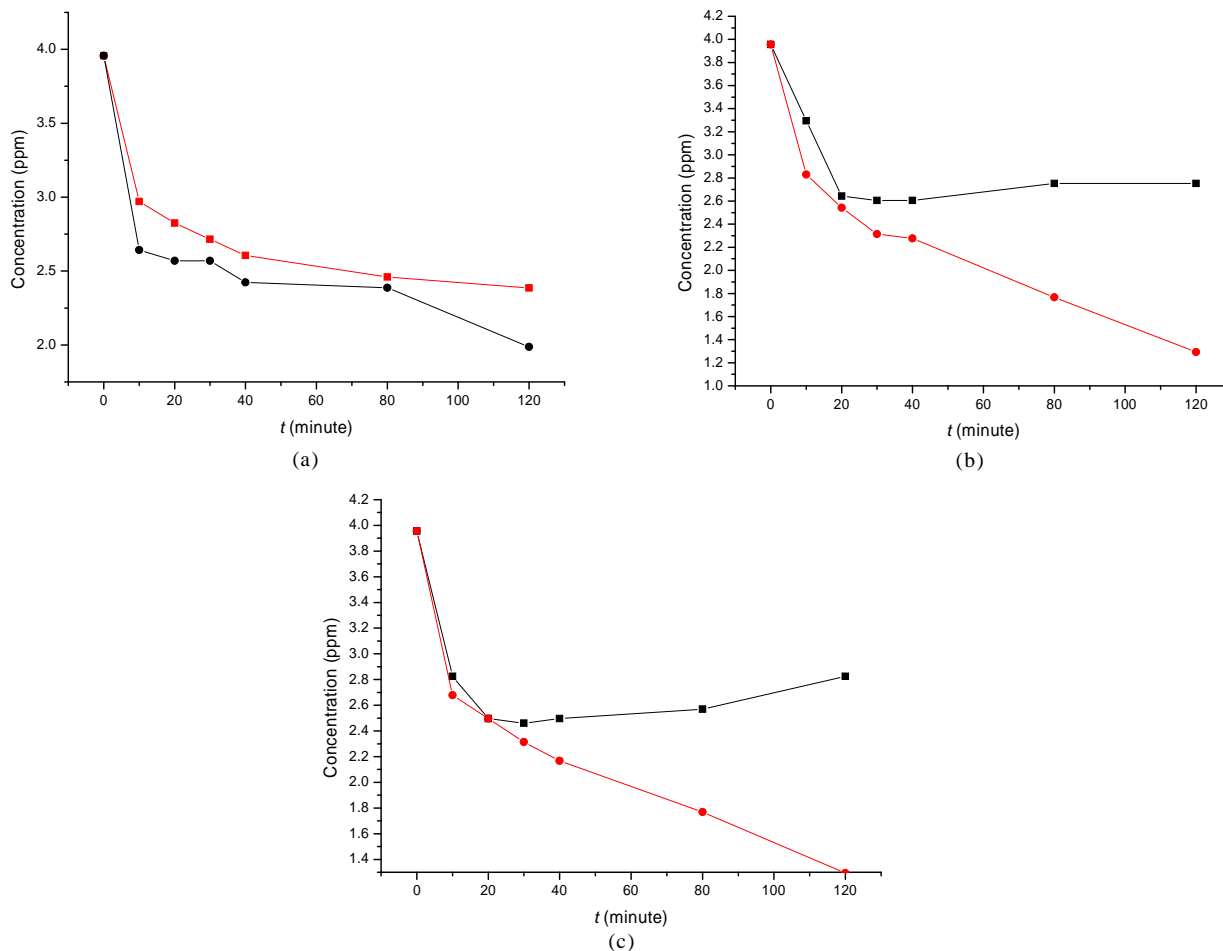| $Sn_{1-x}Co_xO_2$, x =	Reaction Order	UV light		Visible light	
		k	R^2	k	R^2
0	0	0.00683	0.57239	0.01075	0.83697
	1	0.00481	0.63375	0.00927	0.93244
	2	0.00366	0.70187	0.00913	0.95211
0.0025	0	0.00655	0.52151	0.01504	0.85657
	1	0.00466	0.57094	0.01750	0.96809
	2	0.00366	0.63328	0.02735	0.99514
0.005	0	0.00786	0.62716	0.01307	0.81567
	1	0.00607	0.72654	0.01687	0.96418
	2	0.00518	0.83113	0.03153	0.98390

Fig. 3: The plot of the time of irradiation vs. MO concentration after the degradation under UV light (black line) and visible light (red line) using the catalysts of $Sn_{1-x}Co_xO_2$ with x = 0 (a), 0.0025 (b) and 0.005 (c).

Table 6: MO photodegradation kinetics with $Sn_{1-x}Co_xO_2$ catalysts under UV and visible light.

Light source	$Sn_{1-x}Co_xO_2$, x =	k_{obs} (minute^{-1})	k (minute^{-1})
UV	0	0.00366	0.004738
	0.0025	0.00366	0.006078
	0.005	0.00518	0.015638
Visible	0	0.00913	0.011818
	0.0025	0.02735	0.034169
	0.005	0.01687	0.050930

Table 7: Reaction rate of MO photodegradation using $Sn_{1-x}Co_xO_2$ under UV and visible lights.

$Sn_{1-x}Co_xO_2$, x =	Reaction rate (ppm^2.minute^{-1})	
	UV light	Visible light
0	$7.4157 \cdot 10^{-2}$	$1.8497 \cdot 10^{-1}$
0.0025	$9.5130 \cdot 10^{-2}$	$5.3480 \cdot 10^{-1}$
0.005	$24.4758 \cdot 10^{-2}$	$7.9713 \cdot 10^{-1}$

under UV and visible light are relatively similar. However, for $Sn_{1-x}Co_xO_2$ with x = 0.0025 and 0.005 catalysts the reaction rates are significantly different. The photodegra-dation rate constant in visible light has a greater value than that of UV light. This means that the $Sn_{1-x}Co_xO_2$ catalysis is effectively working under visible light. The rate of reaction is determined using equation as follows:

$$r = kC^n \qquad \ldots(9)$$

Where, r is the photodegradation reaction rate, k is the photodegradation rate constant, C is the initial concentration of MO, and n is the photodegradation reaction order. The reaction rate of MO photodegradation is listed in Table 7. The reaction rate of MO degradation under visible light is almost three time faster than that of under UV light.

CONCLUSIONS

The $Sn_{1-x}Co_xO_2$ photocatalysts have been prepared by impregnation method. The cobalt may be recognized by means of the larger lattice parameters of the $Sn_{1-x}Co_xO_2$ with the increase of cobalt. Optical absorption studies clearly indicate the visible light response with the existence of cobalt. A higher photocatalytic activity for the decomposition of MO in the visible region has been confirmed for the prepared $Sn_{1-x}Co_xO_2$ sample compared to the pure SnO_2.

ACKNOWLEDGEMENT

REFERENCES

Alves de Lima, R. O., Bazo, A. P., Salvadori, D.M.F., Rech, C.M., de Palma Oliveira, D. and de Arago Umbuzeiro, G. 2007. Mutagenic and carcinogenic potential of a textile azo dye processing plant effluent that impacts a drinking water source. Mutation Research-Genetic Toxicology and Environmental Mutagenesis, 626(1-2): 53-60.

Banerjee, S., Pillai, S.C., Falaras, P., O'Shea, K.E., Byrne, J.A. and Dionysiou, D.D. 2014. New insights into the mechanism of visible light photocatalysis. The Journal of Physical Chemistry Letters, 5(15): 2543-2554.

Barakat, N.A., Khil, M.S., Sheikh, F.A. and Kim, H.Y. 2008. Synthesis and optical properties of two cobalt oxides (CoO and Co_3O_4) nanofibers produced by electrospinning process. The Journal of Physical Chemistry C, 112(32): 12225-12233.

Carmen, Z. and Daniel, S. 2012. Textile organic dyes-characteristics, polluting effects and separation/elimination procedures from industrial effluents - a critical overview. In: Organic Pollutants Ten Years After the Stockholm Convention - Environmental and Analytical Update.

Cerri, J.A., Leite, E.R., Gouvêa, D., Longo, E. and Varela, J.A. 2005. Effect of cobalt(II) oxide and manganese(IV) oxide on sintering of tin(IV) oxide. Journal of the American Ceramic Society, 79(3): 799-804.

Cisneros, R.L., Espinoza, A.G. and Litter, M.I. 2002. Photodegradation of an azo dye of the textile industry. Chemosphere, 48(4): 393-399.

De Almeida, R.M., Souza, F.T.C., Júnior, M.A.C., Albuquerque, N.J. A., Meneghetti, S.M.P. and Meneghetti, M.R. 2014. Improvements in acidity for TiO_2 and SnO_2 via impregnation with MoO_3 for the esterification of fatty acids. Catalysis Communications, 46: 179-182.

Ito, T., Adachi, Y., Yamanashi, Y. and Shimada, Y. 2016. Long term natural remediation process in textile dye polluted river

sediment driven by bacterial community changes. Water Research, 100: 458-465.

Jäger, I., Hafner, C., Welsch, C., Schneider, K., Iznaguen, H. and Westendorf, J. 2006. The mutagenic potential of madder root in dyeing processes in the textile industry. Mutation Research - Genetic Toxicology and Environmental Mutagenesis, 605(1-2): 22-29.

LeVan, M.D. and Vermeulen, T. 1981. Binary Langmuir and Freundlich isotherms for ideal adsorbed solutions. Journal of Physical Chemistry, 85(22): 3247-3250.

Li, Y.Z., Sun, C.F. and Yang, L.P. 2013. Structures and spectroscopic properties of three aromatic heterocyclic dye photosensitizers. Journal of Theoretical & Computational Chemistry, 12(6): 1-12.

Ohtani, B. 2010. Photocatalysis A to Z - what we know and what we do not know in a scientific sense. Journal of Photochemistry and Photobiology C: Photochemistry Reviews, 11(4): 157-178.

Ohtani, B. 2011. Photocatalysis by inorganic solid materials: Revisiting its definition, concepts, and experimental procedures. Advances in Inorganic Chemistry, 63: 395-430.

Ozdemir, S., Cirik, K., Akman, D., Sahinkaya, E. and Cinar, O. 2013. Treatment of azo dye-containing synthetic textile dye effluent using sulfidogenic anaerobic baffled reactor. Bioresource Technology, 146: 135-143.

Patil, P.S., Kadam, L.D. and Lokhande, C.D. 1996. Preparation and characterization of spray pyrolysed cobalt oxide thin films. Thin Solid Films, 272(1): 29-32.

Prodjosantoso, A.K., Kusumawardani, K., Pranjoto, U. and Handoko, C.T. 2017a. Synthesized and chracterization of $Ca_{1-x}Co_xTiO_3$ and its photocatalytic activity on photodegradation of methylene blue. Asian J. Chem., 29(6): 1270-1274.

Prodjosantoso, A.K., Rahmawati, T. and Kusumawardani, C. 2017b. Tin(IV) oxide-supported cobalt oxides catalysts for methylene blue photodegradation. Research Journal of Chemistry and Environment, 21(12): 12-20.

Reimann, K. and Steube, M. 1998. Experimental determination of the electronic band structure of SnO_2. Solid State Communications, 105(10): 649-652.

Ribeiro, A.R. and Umbuzeiro, G. de A. 2014. Effects of a textile azo dye on mortality, regeneration, and reproductive performance of the planarian, *Girardia tigrina*. Environmental Sciences Europe, 26(1): 22.

Robinson, T., Chandran, B. and Nigam, P. 2002. Removal of dyes from a synthetic textile dye effluent by biosorption on apple pomace and wheat straw. Water Research, 36(11): 2824-2830.

Samad, A., Furukawa, M., Katsumata, H., Suzuki, T. and Kaneco, S. 2016. Photocatalytic oxidation and simultaneous removal of arsenite with CuO/ZnO photocatalyst. Journal of Photochemistry and Photobiology A: Chemistry, 325: 97-103.

Vidal, J., Villegas, L., Peralta-Hernández, J.M. and Salazar González, R. 2016. Removal of Acid Black 194 dye from water by electrocoagulation with aluminum anode. Journal of Environmental Science and Health, Part A, 51(4): 289-296.

Viter, R., Katoch, A. and Kim, S.S. 2014. Grain size dependent bandgap shift of SnO_2 nanofibers. Metals and Materials International, 20(1): 163-167.

Yang, L. and Kruse, B. 2004. Revised Kubelka Munk theory. I. Theory and application. Journal of the Optical Society of America, 21(10): 1933-1941.

Zheng, Y., Luo, C., Liu, L., Yang, Z., Ren, S., Cai, Y. and Xiong, J. 2016. Synthesis of hierarchical TiO_2/SnO_2 photocatalysts with different morphologies and their application for photocatalytic reduction of Cr(VI). Materials Letters, 181: 169-172.